Selective Determination of Acenaphthene in Mixtures of Three-Ring Polycyclic Aromatic Hydrocarbons by Fluorescence Quenching in Micellar Medium of Cetylpyridinium Bromide

Juan H. Ayala,[1] Ana M. Afonso,[1] and Venerando González Díaz[1,2]

The interaction of acenaphthene, anthracene, and phenanthrene with cetylpyridinium bromide (CPB) was studied. The CPB acts as a quencher provoking inhibition of fluorescence intensity emitted by these hydrocarbons. The existing differences in the fluorescence inhibition for these PAHs allow us to develop a selective synchronous spectrofluorimetric method for the determination of acenaphthene in a CPB micellar medium, with a detection limit of 9.2 and 10.4 ng · ml^{-1} for $\Delta\lambda = 10$ and 40 nm, respectively. The method was applied to the selective determination of acenaphthene in mixtures of typical three-ring hydrocarbons, including anthracene, phenanthrene, and fluorene.

KEY WORDS: Micelles; three-ring polycyclic aromatic hydrocarbons; quenching.

INTRODUCTION

Three-ring polycyclic aromatic hydrocarbons, such as anthracene, phenanthrene, fluorene, and acenaphthene, are well known to be principal constituents of polycyclic aromatic hydrocarbons (PAH) originating in fossil fuel. These three-ring PAHs have become of considerable interest in industrial and environmental analytical chemistry because they occur as impurities in coal-derived products and as pollutants in the biosphere.[1,2]

Synchronous fluorescence (SF) methods are more selective than ordinary fluorescence methods for the analysis of mixtures. SF has been used to characterize crude and refined oils[3-5] and to identify and determine polycyclic aromatic hydrocarbons.[6-12] Several synchronous spectra of typical three-ring compounds have been characterized along with other polyaromatic compounds.[13]

Analytically, micellar media are useful because their presence can improve the sensitivity and selectivity of many luminescence determinations. The use of selective fluorescence quenching agents further simplifies observed emission spectra by eliminating signals from undesired chemical interferences having only slightly different molecular structures. However, there are few studies of fluorescence quenching in micellar medium when the surfactant acts, furthermore, as quencher. The use of cetylpyridinium bromide as a selective quencher for polycyclic aromatic hydrocarbons was reported by Ayala *et al.*[14,15].

In a former paper[16] the interaction of fluorene and cetylpyridinium bromide (CPB) was studied and a selective synchronous spectrofluorimetric method for determination of fluorene in a CPB micellar medium was

[1] Department of Analytical Chemistry, Nutrition and Food Science, University of La Laguna, Campus de Ancheta, Astrofísico Francisco Sánchez s/n, E-38201 La Laguna, Spain.
[2] To whom correspondence should be addressed.

Table I. Conventional Spectrofluorimetric Characteristics of Anthracene, Phenanthrene, and Acenaphthene in Different Media

Three-ring PAH	Aqueous medium[a]			Micellar medium[b]		
	λ_{ex} (nm)	λ_{em} (nm)	I_F	λ_{ex} (nm)	λ_{em} (nm)	I_F
Acenaphthene	225[c]	321	450.9	292	321	31.0
	290	335			335	
					352	
Anthracene	250, 325	379	622.0	326	378	10.4
	340, 357	401		337	400	
	377	424		358	422	
Phenanthrene	211, 250	346	218.6	284	346	6.4
	275, 292	363		293	363	
	324	383		323	383	

[a] $C_{PAH} = 2.0 \cdot 10^{-7} M$.
[b] $C_{PAH} = 4.0 \cdot 10^{-6} M$.
[c] The boldface values correspond to the excitation and emission maxima.

Table II. Micellar Inhibition Factors, Analytical Sensitivities, and CPB Concentrations to Reach an Inhibition of 90%

Three-ring PAH	MIF	Analytical sensitivity		$(C_{CPB})_{90} \cdot 10^4 M$
		Aqueous	Micellar	
Acenaphthene	148.6	2199.3	14.8	8.6
Anthracene	800.0	1768.0	2.2	4.0
Phenanthrene	406.5	573.2	1.4	4.9

established. In the present work conventional and synchronous spectrofluorimetric characteristics of acenaphthene, anthracene and phenanthrene in a micellar medium of CPB are established. The quenching processes, which take place between these three-ring PAHs and cetylpyridinium bromide, are established. By using CPB micelles, a selective method for determination of acenaphthene in the presence of anthracene, phenanthrene, and fluorene by synchronous spectrofluorimetry is proposed.

EXPERIMENTAL

Apparatus. Fluorescence measurements were made with a Perkin–Elmer LS-50 luminescence spectrometer equipped with a xenon discharge lamp and connected via an RS232C interface to an Epson PCAX2e computer. The control of the spectrometer was accomplished using Fluorescence Data Manager software. The fluorescence measurements were made in standard 1 × 1-cm quartz cells, thermostatted at 25 ± 0.1°C with a Selecta Frigitherm S 382 ultrathermostat.

Contour maps were obtained by the elaboration of a Basic program within the OBEY application of the Fluorescence Data Manager software. This program allows successive scanning of several emission or synchronous spectra with different excitation wavelengths or $\Delta\lambda$, respectively, and transforms them into a matrix of experimental data. The file containing this matrix is used as input in a commercial program SURFER to obtain contour maps.

Reagents and Solutions. A stock solution ($10^{-3} M$) of acenaphthene, anthracene, phenanthrene, and fluorene (Aldrich) was prepared in ethanol (Merck). Working solutions were prepared by appropriate dilution with ethanol. A stock solution ($5 \cdot 10^{-2} M$) of cetylpyridinium bromide (CPB) (Sigma Chemical Co.) was prepared in deionized water. All chemicals used were of analytical reagent grade.

General Procedure for the Determination of Acenaphthene. To an aliquot containing 0.31–15.40 or 0.31–18.50 μg of acenaphthene, for $\Delta\lambda$ = 10 and 40 nm, respectively, in a 25-ml calibrated flask, add 1.3 ml of a $5 \cdot 10^{-2} M$ CPB solution and the necessary volume of ethanol so that the final solution contains 0.5% (v/v) of organic solvent, and dilute to volume with deionized water. The fluorescence intensity measures are made at synchronous maxima of acenaphthene $\lambda^0_{s,ex}$ = 310 nm ($\Delta\lambda$ = 10 nm) and $\lambda^0_{s,ex}$ = 295 nm ($\Delta\lambda$ = 40 nm). Calibration graphs are obtained from standard solutions prepared under the same experimental conditions.

General Procedure for the Determination of Acenaphthene in Mixtures of Three-Ring PAHs. An aliquot containing acenaphthene, anthracene, phenanthrene, and fluorene at the allowed ratios is analyzed according to the above method.
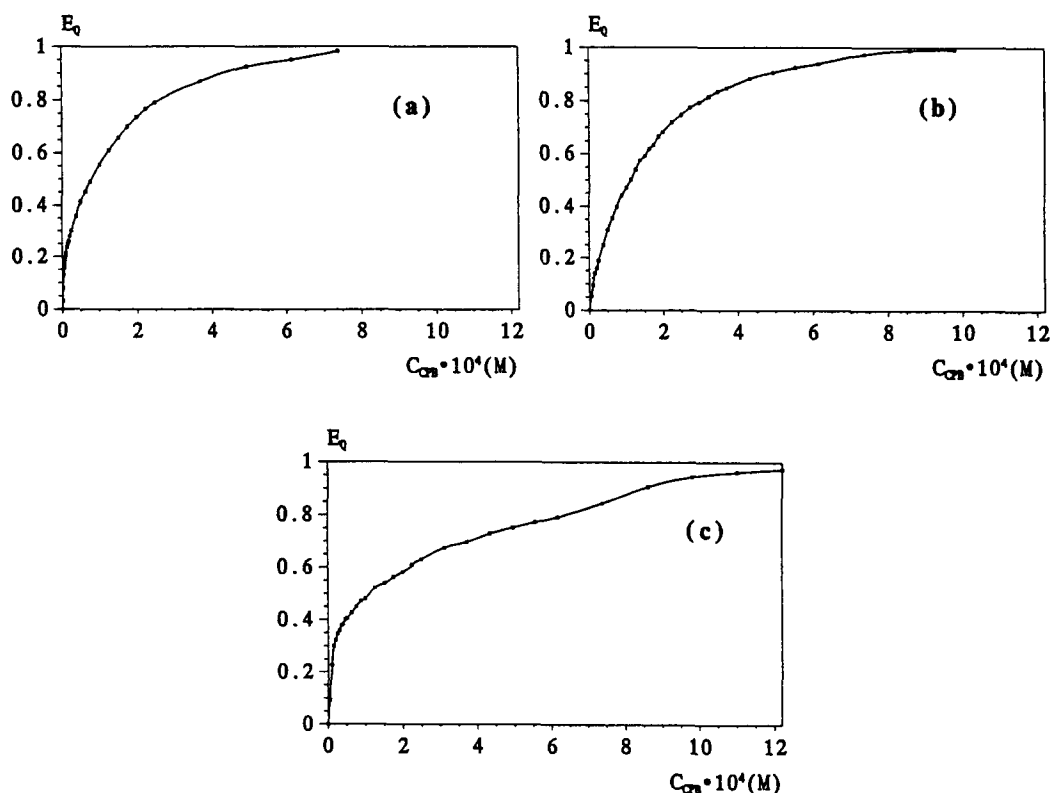
Fig. 1. Influence of the CPB concentration in the efficiency of the quenching of $2 \cdot 10^{-7}$ M anthracene (a), $4 \cdot 10^{-7}$ M phenanthrene (b), and $4 \cdot 10^{-7}$ M acenaphthene (c).

RESULTS AND DISCUSSION

Spectrofluorimetric Characteristics

Conventional Fluorescence. Polycyclic aromatic hydrocarbons are slightly soluble in water. In order to study the spectrofluorimetric behavior of acenaphthene, anthracene, and phenanthrene, ethanol–water solutions were used. We refer to aqueous solutions as containing 0.5% (v/v) ethanol–water. Solutions containing the same volume of ethanol and $2.6 \cdot 10^{-3}$ M CPB, to ensure a surfactant concentration greater than its critical micellar concentration (cmc) $(7.32 \cdot 10^{-4}$ $M)$, are referred to as micellar solutions. This cmc value was determined conductimetrically under similar experimental conditions to those used in fluorescence measurements. Table I shows the main differences of excitation and emission spectra, in both media, for the three three-ring PAHs considered.

In relation to the aqueous medium, the excitation spectra in the micellar medium present a considerable simplification, especially due to the practical disappearance of the bands or excitation peaks to $\lambda_{ex} \leq 280$ nm. Upon comparing the wavelengths of the excitation max-

ima, important bathochromic shifts (between 43 and 87 nm) are observed on passing from an aqueous to a micellar medium, while the respective values of the emission maxima do not experience important changes. It also emphasizes the great inhibition observed in the fluorescence intensity emitted by hydrocarbons in the micellar medium.

In order to quantify the effect of the micellar medium of CPB in the inhibition of the fluorescence emitted by the three-ring PAHs, the micellar inhibition factor (MIF)[14] has been used. The MIF value represents the relationship between the slopes of the calibration graphs in both media, that is, the relationship between the analytical sensitivity in aqueous medium with respect to that of micellar medium. The MIF values included in Table II show the intensity of the inhibition processes.

The comparison of the analytical sensitivities in each medium allows us to explain the effect of the micellar medium of CPB in the inhibition of the fluorescence emitted by three-ring PAHs. Table II shows that the analytical sensitivities of anthracene and phenanthrene are considerably lower than that of acenaphthene in micellar medium. The last hydrocarbon presents im-
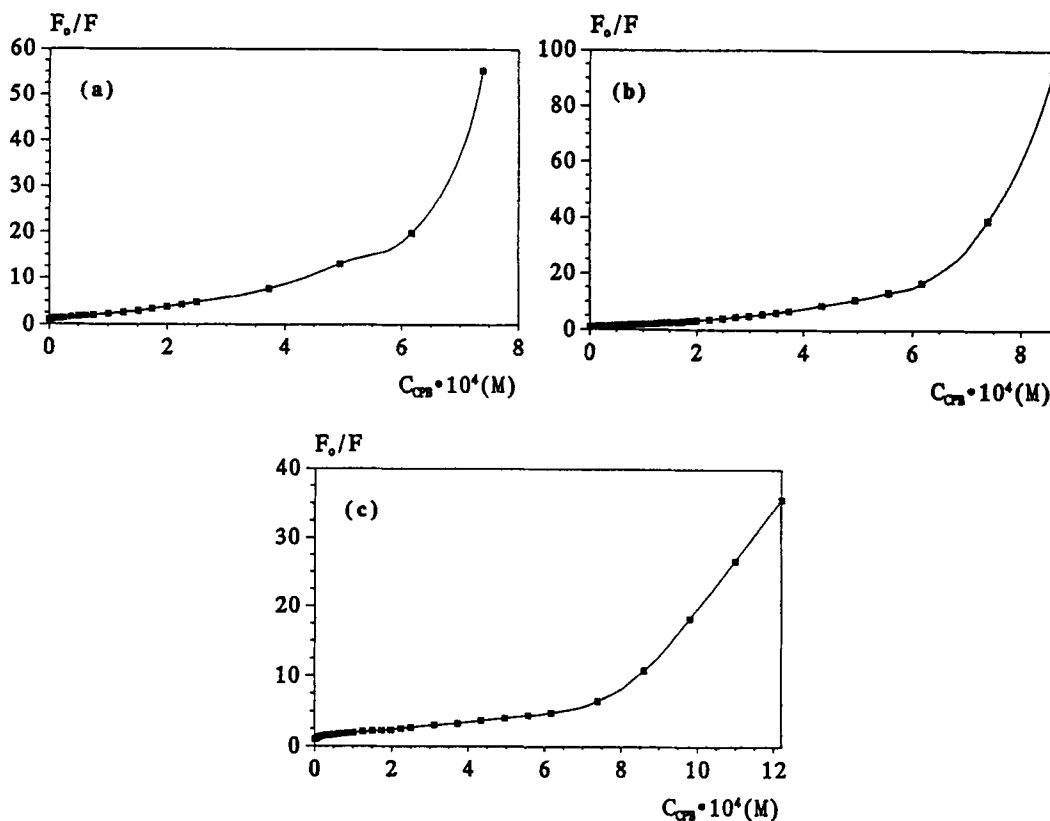
Fig. 2. Stern–Volmer plots for the quenching of three-ring PAHs by cetylpyridinium bromide: (a) anthracene, (b) phenanthrene, and (c) acenaphthene.

portant analytical sensitivities in the presence of CPB micelles, in spite of showing a strong decrease in the emitted fluorescence intensity.

Synchronous Fluorescence. The introduction of a micellar medium of CPB produces different degrees of inhibition in the fluorescence emitted by the three-ring PAHs considered. Moreover, the use of analytical techniques as synchronous spectrofluorimetry can contribute to improve the selectivity of the analytical determination.

The main difficulty to resolve mixtures by synchronous spectrofluorimetry lies in knowing previously the optimum value or values of $\Delta\lambda$ which allow determination of each component in a selective way.

The optimum values of $\Delta\lambda$ can be selected through the contour maps obtained from conventional spectra. However, it can be better the use of synchronous contour maps[4,17] which supply more selective information.

The values of $\Delta\lambda$ that produce the maximum intensity peak of the synchronous spectra are 30 nm ($\lambda^0_{s,ex}$ = 292 nm), 50 nm ($\lambda^0_{s,ex}$ = 356 nm), and 60 nm ($\lambda^0_{s,ex}$ =

294 nm) for acenaphthene, anthracene, and phenanthrene, respectively.

Fluorescence Quenching by CPB

The inhibitions of the fluorescence intensity, which vary in a regular way with the quencher concentration, can be considered typical of quenching processes. The efficiency of a quenching process is a measure of the inhibition that the fluorescence intensity emitted by a fluorophore experiences in the presence of a given quencher concentration. It can also represent the necessary quencher concentration to produce a fixed decrease preset in the fluorescence of a fluorophore. In our case, we have established the efficiency of the quenching in relative terms,[18] by the equation

$$E_Q = 1 - \frac{F}{F_0}$$

where F and F_0 represent the fluorescence intensity emit-

Table III. Values of Quenching Constants of Three-Ring PAHs by Cetylpyridinium Bromide

Three-ring PAH	$[CPB] \cdot 10^4\ M$	$K \cdot 10^{-3}\ M^{-1}$	Intercept	r
Acenaphthene	<6.17	$K_{Sv} = 5.37 \pm 0.05$	1.39	0.999
		$K_D = 4.76 \pm 0.03$	1.42	0.999
		$V = 0.14$		
	>6.17	$K_s = 3.50 \pm 0.17$	−0.62	0.996
Anthracene	<1.5	$K_{Sv} = 11.51 \pm 0.14$	1.14	0.999
	<6.17	$K_D = 6.19 \pm 0.05$	1.18	0.999
		$V = 2.23$		
Phenanthrene	<1.12	$K_{Sv} = 8.83 \pm 0.08$	1.01	0.999
	<6.17	$K_D = 4.90 \pm 0.02$	1.03	0.999
		$V = 2.26$		

ted for each hydrocarbon in the presence and absence of quencher, respectively.

Figure 1 shows a plot of E_Q versus CPB concentration for the three three-ring PAHs considered. To CPB concentrations higher than $10^{-3}\ M$, fluorescence inhibitions that exceed 95% are reached. Table II shows the necessary surfactant concentration to reach inhibitions of 90%, $(C_{CPB})_{90}$. It is observed that except for acenaphthene, such concentrations are lower to the cmc of the CPB.

To determine the interactions involved in the quenching of three-ring PAHs by CPB, Stern–Volmer plots were obtained (Fig. 2). The analysis of these curves shows that at CPB concentrations lower than $6.17 \cdot 10^{-4}$, $1.5 \cdot 10^{-4}$, and $1.12 \cdot 10^{-4}\ M$ for acenaphthene, anthracene, and phenanthrene, respectively, we obtained good relationships ($r = 0.999$) between F_0/F and CPB concentration. A linear Stern–Volmer plot is indicative that a single mechanism is involved in the quenching process, which could be either dynamic or static in nature. In the case of acenaphthene, the intercept is distant from one because, at the lowest CPB concentrations, the fluorescence must be modified by mechanisms other than quenching.[15,19]

At CPB concentrations higher than those said before, positive deviations of linearity was observed, which suggest that quenching is a combination of both dynamic and static quenching processes.[20–22] The loss of the Stern–Volmer equation linearity is because only a part of the three-ring PAHs molecules is deactivated by collisional mechanisms, while the rest form complex three-ring PAHs*CPB in the ground state. The different models developed to explain this instantaneous phenomenon (static quenching) lead to a modified form of the Stern–Volmer equation.[20]

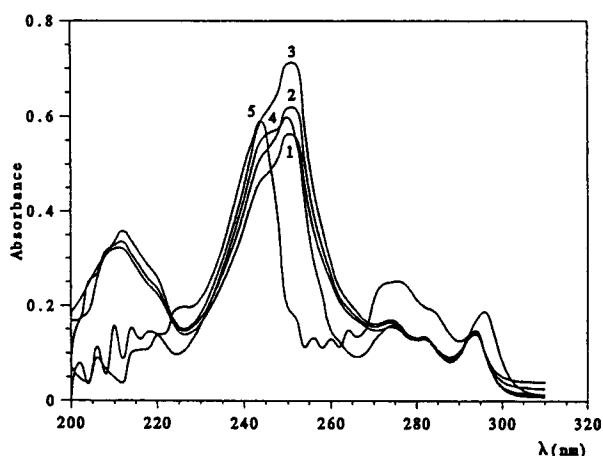$$F_0/Fe^{V[Q]} = (1 + K_D\ [Q]) \qquad (1)$$

Fig. 3. Absorption spectra of $2 \cdot 10^{-5}\ M$ phenanthrene in the presence of different concentrations of CPB: (1) 0 M, (2) $2 \cdot 10^{-4}\ M$, (3) $3 \cdot 10^{-4}\ M$, (4) $6 \cdot 10^{-4}\ M$, and (5) $1.5 \cdot 10^{-3}\ M$.

where V is the constant of static quenching, K_D represents the dynamic aspects of the deactivation of the three-ring PAHs excited state, and $[Q]$ is the CPB concentration.

For the treatment of the experimental data, values of V are given until a linear plot of $F_0/Fe^{V[Q]}$ versus CPB concentration is obtained ($r = 0.999$). The V value, which results in the most linear plot, is the static quenching constant, while the slope of the straight lines obtained represents dynamic quenching constant. The values obtain for K_D and V are shown in Table III.

The previously applied model presents important deviations of linearity a CPB concentrations above cmc, possibly due to the incorporation of PAHs in the hydrophobic core of the micelles, which practically prevents the possibility of dynamic quenching.

From Eq. (1), substituting V by the static quenching constant (K_s) and applying napierian logarithms, we ob-
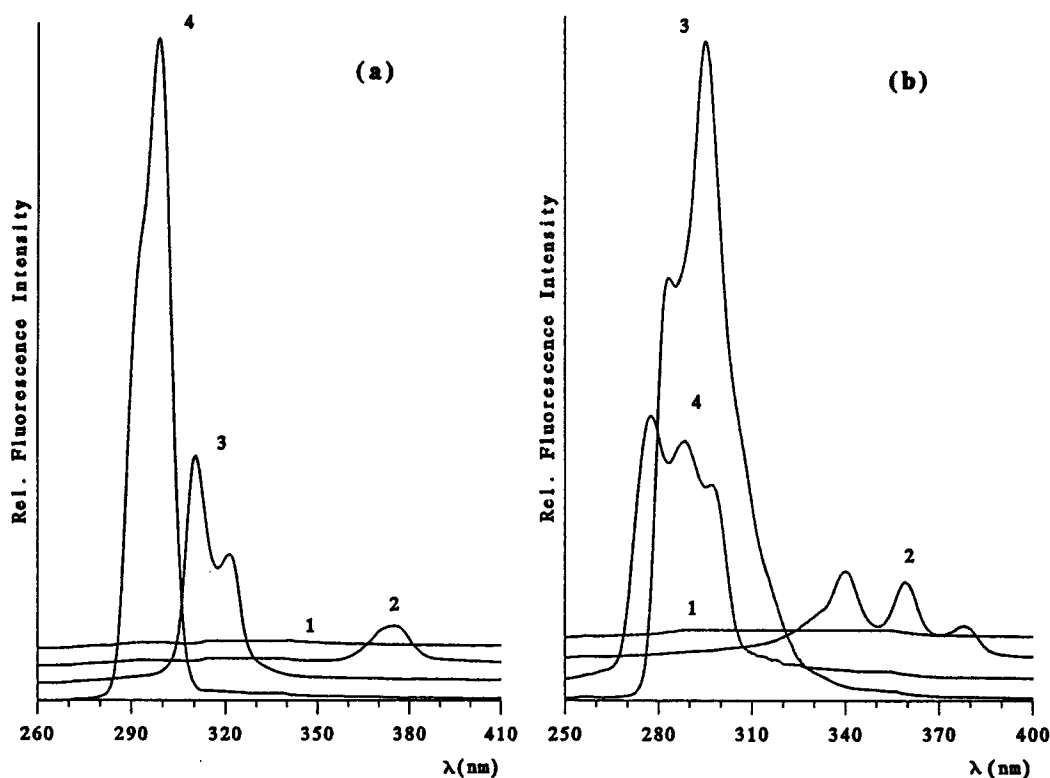
Fig. 4. Synchronous spectra at $\Delta\lambda = 10$ nm (a) and $\Delta\lambda = 40$ nm (b) of phenanthrene (1), anthracene (2), acenaphthene (3), and fluorene (4) in a micellar medium of CPB. $C_{PAH_2} = 2 \cdot 10^{-6}\ M$; $C_{CPB} = 2.6 \cdot 10^{-3}\ M$; Slits, 5–6 nm.

tained

$$\ln (F_0/F) = \ln (\tau_0/\tau) + K_s [Q] \qquad (2)$$

The above equation shows that when the τ_0/τ ratio becomes constant, then a plot of $\ln(F_0/F)$ versus CPB concentration becomes linear and only static quenching exists. This representation allows the calculation of K_s and of the $\ln(\tau_0/\tau)$.

The high values of the MIF for anthracene and phenanthrene produce slightly reliable F_0/F values. For this reason, Eqs. (2) has been applied only to acenaphthene.

Upon plotting Eqs. (2), we obtain the values of $(3.50 \pm 0.17) \cdot 10^3\ M^{-1}$ for K_s and -0.62 for the intercept. This value of K_s should be taken as the association constant between acenaphthene and CPB micelles.

If in the range of CPB concentrations considered, there is static quenching, the τ_0/τ relationship would be equal to one; consequently, the intercept would be zero. The value obtained (-0.62) different from zero has to take into account that dynamic and/or static quenching processes are produced below the lowest concentration limit in this zone. Furthermore, the negative value could

Table IV. Determination of Acenaphthene in the Presence of Other Three-Ring PAHs: $C_{Acenaphthene} = 123.39$ ng · ml^{-1}

Interference	Ratio, Acenaph.: Interf.	Acenaphthene found (ng · ml^{-1})[a]	
		$\Delta\lambda = 10$ nm	$\Delta\lambda = 40$ nm
Anthracene	1:2	127.97 (3.7%)	128.79 (4.4%)
	1:5	120.78 (−2.1%)	121.65 (−1.4%)
	1:10	115.15 (−6.7%)	115.84 (−6.1%)
Phenanthrene	1:2	131.30 (6.4%)	130.81 (6.0%)
	1:5	125.74 (1.9%)	123.14 (−0.2%)
	1:10	130.56 (5.8%)	125.74 (1.9%)
Fluorene	1:1	118.81 (−3.1%)	145.05 (17.6%)
	1:2	123.39 (0%)	176.10 (42.7%)
	1:5	130.25 (5.6%)	251.63 (103.9%)

[a]Values in parentheses refer to the error obtained in the determination.

be related to the higher stabilization of the singlet excited state of acenaphthene in micellar medium than in solutions with CPB concentrations below the cmc, which could produce τ_0/τ ratios below one.

A method to differentiate dynamic and static quenching processes consists of studying the absorption

spectra of the fluorophores in solutions with variable quencher concentrations. The different hydrocarbons present a similar behavior. Figure 3 shows the absorption spectra of phenanthrene. The displacement in the absorption maxima at high CPB concentrations would explain the formation of complexes in the ground state between the fluorophore and the quencher, and so, it must be associated with static quenching processes. On the contrary, as collisional quenching affects only the excited state of the fluorophore, it is to be expected that changes are not produced in the absorption spectra, as it occurs at low CPB concentrations.

Analytical Considerations

To develop a procedure for the determination of acenaphthene, the analytical characteristics of the synchronous spectra recorded using $\Delta\lambda$ = 10 nm and $\Delta\lambda$ = 40 nm were evaluated. These $\Delta\lambda$ values have been selected to reach the best conditions of sensitivity and selectivity in the determination of acenaphthene.

In the presence of CPB, linear calibration graphs with high correlation coefficients of 0.9998 and 0.9996 were obtained by plotting the fluorescence intensity measures on the synchronous spectra ($\lambda^0_{s,ex}$ = 310 and 295 nm) against the acenaphthene concentration for $\Delta\lambda$ = 10 nm and $\Delta\lambda$ = 40 nm, respectively. The linear concentration ranges are 12.3–617.0 ng·ml^{-1} ($\Delta\lambda$ = 10 nm) and 12.3–740.4 ng·ml^{-1} ($\Delta\lambda$ = 40 nm) and the detection limits[21] are 9.2 and 10.4 ng·ml^{-1}, respectively.

When the methods were applied to a series of 11 samples containing 308.5 ng·ml^{-1} of acenaphthene, relative errors of ± 1.44 and ± 1.52% and relative standard deviations of 2.01 and 2.26% were obtained for $\Delta\lambda$ = 10 nm and $\Delta\lambda$ = 40 nm, respectively.

In order to apply the proposed method to the selective determination of acenaphthene in synthetic three-ring PAHs mixtures, the spectral interferences were studied under the same experimental conditions as used for acenaphthene. Figure 4a shows that the determination of acenaphthene without interferences of the other hydrocarbons is possible at $\Delta\lambda$ = 10 nm. The use of this $\Delta\lambda$ produces a peak for acenaphthene as an incompletely resolved doublet, which may be more favourable

than a singlet for its characterization in complex mixtures. On the other hand, the use of a $\Delta\lambda$ value of 40 nm (Fig. 4b) produces a higher sensitivity in the determination of acenaphthene but a lower selectivity due to the overlapping that acenaphthene and fluorene spectra present.

Table IV shows the recoveries of acenaphthene in the presence of different concentrations of each of the three-ring PAHs considered.

REFERENCES

1. W. H. Griest and J. E. Caton (1983) *Handbook of Polycyclic Aromatic Hydrocarbons*, Marcel Dekker, New York.
2. T. Vo-Dinh (1989) *Chemical Analysis of Polycyclic Aromatic Compounds*, Wiley–Interscience, New York.
3. J. B. F. Lloyd (1971) *J. Forens. Sci. Soc.* **11**, 235–253.
4. J. B. F. Lloyd (1980) *Analyst* **105**, 97–109.
5. P. John and I. Soutar (1976) *Anal. Chem.* **48**, 520–528.
6. T. Vo-Dinh, R. B. Gammage, A. R. Hawthorne, and J. H. Thorngate (1978) *Environ. Sci. Technol.* **12**, 1297–1302.
7. E. L. Inman and J. D. Winefordner (1982) *Anal. Chem.* **54**, 2018–2022.
8. T. Vo-Dinh, R. B. Gammage, and P. R. Martinez (1981) *Anal. Chem.* **53**, 253–258.
9. M. J. Kerkhoff, T. M. Lee, E. R. Allen, D. A. Lundgren, and J. D. Winefordner (1985) *Environ. Sci. Technol.* **19**, 695–699.
10. L. A. Files, B. T. Jones, S. Hanamura, and J. D. Winefordner (1986) *Anal. Chem.* **58**, 1440–1443.
11. J. J. Santana, Z. Sosa, A. M. Afonso, and V. González (1991) *Anal. Chim. Acta* **255**, 107–111.
12. J. J. Santana, Z. Sosa, A. M. Afonso, and V. González (1992) *Talanta* **39**, 1611–1617.
13. M. Tachibana and M. Furusawa (1994) *Analyst* **119**, 1081–1085.
14. J. H. Ayala, A. M. Afonso, and V. González (1997) *Talanta* **44**, 257–267.
15. J. H. Ayala, A. M. Afonso, and V. González (1997) *Appl. Spectrosc.* (in press).
16. J. H. Ayala, A. M. Afonso, and V. González (1997) *Mikrochim. Acta* (in press).
17. M. T. Oms, R. Forteza, V. Cerda, F. Garcia, and A. L. Ramos (1990) *Int. J. Environ. Anal. Chem.* **42**, 1–14.
18. Y. Kusumoto, M. Shizuka, and I. Satake (1986) *Chem. Lett.* 529–532.
19. B. B. Purdy and R. J. Hurtubise (1992) *Anal. Chem.* **64**, 1400–1404.
20. M. R. Eftink and C. A. Ghiron (1976) *J. Phys. Chem.* **80**, 486–493.
21. W. M. Vaughan and G. Weber (1970) *Biochemistry* **9**, 464–473.
22. J. R. Lakowicz (1983) *Principles of Fluorescence Spectroscopy*, Plenum Press, New York, pp. 257–295.
23. G. L. Long and J. D. Winefordner (1983) *Anal. Chem.* **55**, 712A–724A.